

# The chromospheric response due to filament eruption

**B.P. Filippov**

Institute of Terrestrial Magnetism, Ionosphere and Radio Wave Propagation, Russian Academy of Sciences,  
142092, Troitsk Moscow Region, Russia

Received 4 October 1996 / Accepted 12 December 1996

**Abstract.** Frozen-in motion of chromospheric plasma during an eruption of a filament of inverse polarity is considered. At the initial stage of the filament ascent, magnetic field compresses the chromospheric plasma within two belts disposed bilaterally along a polarity inversion line. Compression should be accompanied by heating of plasma and enhancement of emission in  $H\alpha$ . The distance between the belts increases as the filament ascends. The estimates show that this mechanism can be effective to represent the  $H\alpha$  flare kernels dynamics in two-ribbon flares.

**Key words:** Sun: chromosphere – Sun: filaments – Sun: magnetic fields

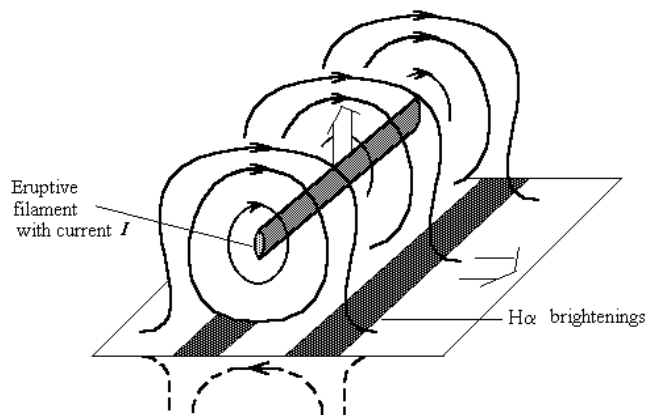


**Fig. 1.** Schematic representation of the magnetic configuration and position of flare ribbons therein

## 1. Introduction

Sudden loss of the filament equilibrium and its fast ascent (eruption) are assumed to be connected with the instability of a magnetic configuration surrounding the filament. An example of such configuration is a model of an inverse polarity filament (Van Tend & Kuperus 1978; Molodenskij & Filippov 1987; Martens & Kuin 1989) in which cold dense matter is supported in the corona by the repulsion of a filament current from currents induced on the surface of the photosphere. The vertical component of subphotospheric magnetic field keeps a filament above a polarity inversion line (“neutral line”) while the horizontal component presses it to the photosphere. These circumstances enable the configuration to store magnetic energy exceeding gravitational energy of the filament (Molodenskij & Filippov 1992). Increase of the filament current leads to the rise of the equilibrium height. But if the background field falls with height sufficiently abruptly (more than  $1/h$ ) (Van Tend & Kuperus 1978), such smooth evolution is possible only until the current value reaches the critical magnitude. Then catastrophe occurs, the equilibrium is violated and the filament ascends.

In the vicinity of ascending filament in the region where magnetic energy predominates over thermal energy of the coronal matter, the magnetic field of the filament sweeps out the

corona, forming a cavity. On the outside boundary of this region, a compressed envelope arises (Filippov & Shilova 1995; Filippov 1996). This scenario corresponds to the development of coronal mass ejection which very often or, possibly, always accompanies a filament eruption. The purpose of this paper is to analyze the response in the chromosphere beneath the filament caused by the filament eruption.

Observations show that filament eruption is linked, as a rule, with a two-ribbon flare (Zirin & Lackner 1969; Martin & Ramsay 1972). There are different opinions in respect to a dilemma what is the cause and what is the effect (Hood & Priest 1980; Kuperus & Van Tend 1981; Anzer & Pneuman 1982), but no doubt both of them are results of the magnetic field reconstruction. Soon after the beginning of the fast ascent of a filament, enhanced  $H\alpha$  emission arises in narrow ribbons aligned with the filament along both sides of it. At first, the ribbons are separated by a narrow absorption gap located where the filament was before. Then they diverge with speeds up to tens of kilometers per second (Banin & Fedorova 1970; Svestka 1976) leaving the dark space between them. Usually, the ribbon stops when it reaches a region with strong magnetic fields near large spots and never spreads over the center of a big spot. Diverged ribbons are the bases of a post flare loop arcade (Rust & Bar 1973).

It is a widespread opinion that  $H\alpha$  emission is a secondary process caused by the penetration of particles accelerated in the region of primary energy release at the top of the arcade (Priest 1982). Making no doubt about this possibility, I believe that a more simple scenario can exist in which emission in the ribbons arises from the heating of the chromospheric gas compressed by the changing magnetic field. Released energy is created by the work of the magnetic field during compression of a plasma. Some peculiarities of the magnetic field structure in the model of inverse polarity suggest such behaviour of plasma density and temperature when the filament ascends (Fig. 1).

The distinctive feature of the model is the presence of two regions beneath the filament where magnetic field lines diverge drastically. The behaviour of the field lines is the same as in vicinity of a saddle point. Using the method of mirror images we can conceive the existence of two saddle points below the photosphere. Motion of these points due to field variations would reflect a displacement of peculiar regions of the field. Then frozen-in plasma motion leads to changes in plasma density. During the compression of matter in some regions, work done by magnetic field produces heat. Finally, a fraction of thermal energy would be transformed into radiation.

## 2. Magnetic field of a model

In two-dimensional inverse polarity model, a filament is represented as a straight linear current in equilibrium with the external magnetic field  $B^{\text{ex}}$ . The vector-potential  $A$  of the filament magnetic field has only one component which can be written, taking into account the boundary condition on the photosphere, in the form

$$A_z = \frac{I}{c} \ln \frac{x^2 + (y+h)^2}{x^2 + (y-h)^2}, \quad (1)$$

where  $h$  is the height of the current above the photosphere, the current is directed along the  $z$ -axis while the  $y$ -axis is vertical.

To violate the equilibrium in this system by catastrophic process, it is necessary that the external field decrease steeper than  $1/h$  starting from some height  $h_0$ . The field of a linear dipole (two near-by linear currents flowing in opposite directions) satisfies this condition and is often assumed as an acceptable approximation to the real field. The shortcoming of such a linear dipole is the small scale of its field. Indeed, when the current exceeds a critical value, its magnetic field dominates over the dipole field in the semi-infinite space  $y > 0$ . This ratio does not arise in an active region for the simple reason that there exist the strong fields of sunspots.

Let the external field be the sum of the field of the dipole  $M$  located at a depth  $d$  below a photospheric neutral line and two "charged threads"  $q$  located at a depth  $d_1$  and at a distance  $\pm a$  from the neutral line

$$B_x^{\text{ex}} = M \frac{x^2 - (y+d)^2}{[x^2 + (y+d)^2]^2} + q \left( \frac{x-a}{(x-a)^2 + (y+d_1)^2} - \frac{x+a}{(x+a)^2 + (y+d_1)^2} \right)$$

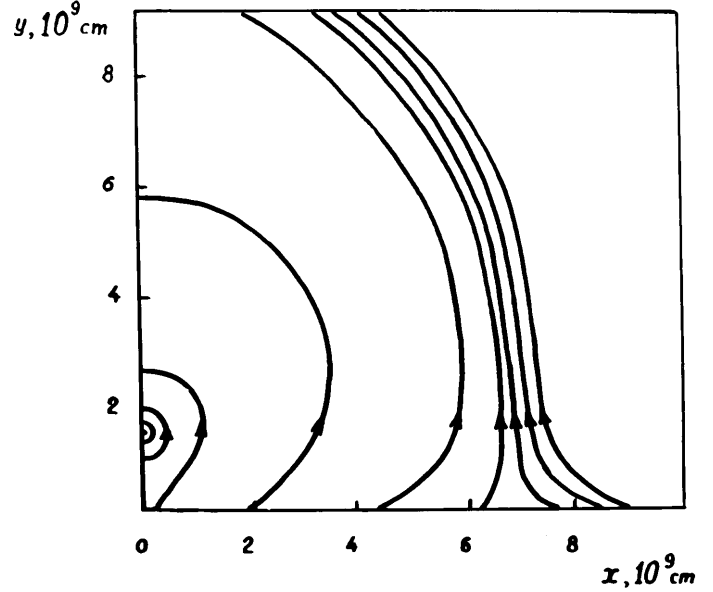


**Fig. 2.** Magnetic field lines of the model at the initial moment of eruption,  $h = 1.6d$ ;  $x$  and  $y$  are in units of  $d = 10^9$  cm. The pattern is symmetric about the  $y$ -axis

$$B_y^{\text{ex}} = M \frac{2x(y+d)}{[x^2 + (y+d)^2]^2} + q \left( \frac{y+d_1}{(x-a)^2 + (y+d_1)^2} - \frac{y+d_1}{(x+a)^2 + (y+d_1)^2} \right). \quad (2)$$

Various ratios between the parameters allow this expression to describe a rather wide variety of fields. The choice of parameters was made for the following reasons.

The field of the charges should present the large-scale part of the external field. The eruption conditions and the initial course of the eruption should be scarcely affected by this part of field. In accordance with this assertion, let  $a = 10d$ . The ratio  $d/d_1$  is approximately equal to the height of the eruption start evaluated as a ratio of spot diameters. It can be assumed as  $2 \div 5$ . It seems to be natural that both components would be turned in the same direction above a polarity inversion line. Then the large scale field increases the stability of the current equilibrium, and there is a maximum value of  $q$  which, when exceeded, enables the eruption.

Catastrophe arises if there are the multiple roots of the equation

$$\frac{I^2}{c^2 y} = \frac{I}{c} \left( \frac{M}{(y+d)^2} - \frac{2qa}{a^2 + (y+d_1)^2} \right), \quad (3)$$

which determines the vertical force balance (the weight of the filament is neglected here). Numerical solution of Eq. (3) shows that instead of  $h = d$  and  $I = Mc/4d$  for the dipole field, eruption starts now when  $h \approx 1.6d$ ,  $I \approx Mc/3.5d$ ,  $q = M/6d^2$ . The onset of the eruption is marked by the fact that the saddle point formed by the dipole and the current field crosses the photospheric plane ( $y = 0$ ) and then rises in the wake of the filament.

Field lines at the chosen parameters are shown in Fig. 2. We should keep in mind that only the field above the photosphere is physically justified in this model. Of course, there are no “dipoles” and “charged threads” below the photosphere but the field above it is the same as if there were. Similarly, the field in the chromosphere at both sides of the filament is like the field in the vicinity of saddle points located below the photosphere. The frozen-in motion of the chromospheric plasma in these two regions leads to compression and heating due to the work of the magnetic field. These regions can be correlated with the flare ribbons. As the current ascends, the saddle points move aside in the initial stage of the process. Then they are brought together as the filament reaches the height  $\sim 10d$ , but by then, the influence of the current on the chromospheric plasma will be negligible. So we can note that the regions with compression are moving apart as the filament ascends. The velocity of the saddle point displacement  $v_s$  varies within wide limits according to the chosen parameters. In a uniform external field, for instance,  $v_s$  can exceed the velocity of the filament ascent  $v_0$ . For the configuration shown in Fig. 2 numerical calculations gives  $v_s \approx 0.3v_0$ .

### 3. Frozen-in chromospheric plasma motion

Above some level in the chromosphere, the magnetic pressure exceeds the gas pressure and plasma motion obeys the magnetic field variations. Any plasma particle in the first approximation is stuck on a field line and moves together with it. General properties of such flows have been considered by Somov and Syrovatskii (1971; 1974). They studied, in particular, the flows in the vicinity of a saddle point, however, their consideration differed from the conditions of our model. Inhomogeneity of the velocity field inevitably leads to formation of regions with plasma compression and rarefaction in accordance with the equation of continuity

$$\frac{\partial \rho}{\partial t} = -\text{div} \rho \mathbf{v}. \quad (4)$$

In the regions of compression, heating will occur (in the case of the adiabatic compression  $\Delta T \sim \Delta \rho^{2/3}$ ).

If a saddle point is located on the surface of the photosphere  $y = 0$  at the point  $x = s$ , the magnetic field in its vicinity can be written in the form

$$\mathbf{B} = G \left( (s - x)\mathbf{e}_x + y\mathbf{e}_y \right), \quad (5)$$

where  $G$  is the field gradient. The speed of the frozen-in motion is

$$\mathbf{v} = c \frac{\mathbf{E} \times \mathbf{B}}{B^2}. \quad (6)$$

The induction electric field  $\mathbf{E}$  is related to the vector potential  $\mathbf{A}$  by the well-known expression

$$\mathbf{E} = -\frac{1}{c} \frac{\partial \mathbf{A}}{\partial t}. \quad (7)$$

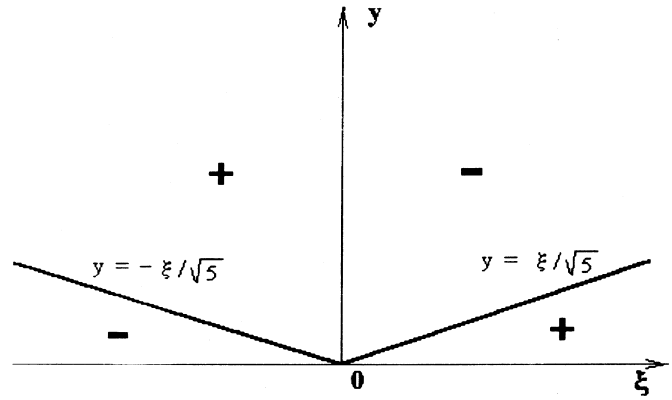


Fig. 3. Regions with compression (-) and rarefaction (+) above the saddle point located on the plane of the photosphere  $y = 0$

Substituting expression (1) into (7) and assuming that only the height  $h$  of the current above the photosphere depends upon time  $t$ , one obtains

$$E_z = -\frac{4Iv_0}{c^2} \frac{y(x^2 + y^2 - h^2)}{(x^2 + y^2 + h^2)^2 - 4y^2h^2}, \quad (8)$$

with  $\partial h / \partial t = v_0$ . In the near-by vicinity of a saddle point  $y \ll x$  and  $y \ll h$ , so

$$E_z = -\frac{4Iv_0}{c^2} \frac{y(x^2 - h^2)}{(x^2 + h^2)^2}, \quad (9)$$

Substituting (9) and (5) into (6) we obtain after derivation with respect to  $x$  and  $y$

$$\text{div} \mathbf{v} = \frac{4Iv_0}{c^3} \frac{\xi(\xi^2 - 5y^2)}{s^2(\xi^2 + h^2)^2}, \quad (10)$$

where the assumption is made that  $x = s \gg h$  and  $\xi = x - s$ .

The sign of  $\text{div} \mathbf{v}$  defines the borders of the regions of compression. It is more obvious if we use a substantial derivative  $D\rho/Dt$  in the equation of continuity (4)

$$\frac{1}{\rho} \frac{D\rho}{Dt} = -\text{div} \mathbf{v}.$$

It can be seen from (10) that there are two regions of compression and two regions of rarefaction above the line  $y = 0$ . The regions are separated by the lines  $\xi = 0$ ,  $y = \pm \xi / \sqrt{5}$  (Fig. 3). The origin of the upper regions is indebted to magnetic field peculiarities: plasma accelerates approaching to the saddle point and decelerates moving away from it. The low regions arises due to the electric field peculiarities:  $E_z$  changes the sign at the line  $y = 0$  producing the divergent and convergent flows.

Fig. 4 shows the distribution of the divergency of the drift velocity  $\text{div} \mathbf{v}$  in the whole domain plotted in Fig. 2. Besides the extremums near the points  $\pm s$ , the extremums close to the saddle point beneath the filament and near the current position are seen. But only the extremums linked with the saddles  $\pm s$  stay for a considerable length of time in the chromosphere.

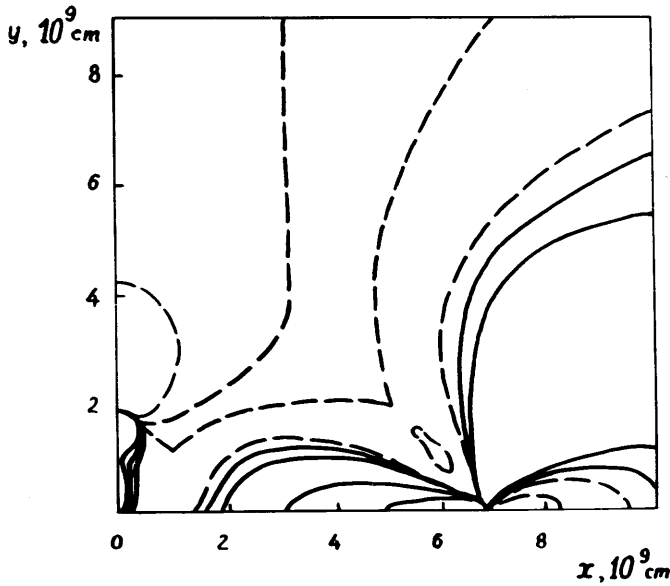


Fig. 4. Distribution of  $\text{div } \mathbf{v}$  at the initial moment of eruption of the inverse polarity filament. The solid curves show  $\text{div } \mathbf{v} \leq 0$ , the dashed curves show  $\text{div } \mathbf{v} > 0$ . The curves represent the levels 0, 0.1, 0.5, 1 in arbitrary units

The discussion so far corresponds to infinitesimal density variations at a given moment. To judge what is the magnitude of compression and consequently the degree of heating, it is necessary to integrate Eq. (4) and to obtain density variation over a finite time interval.

#### 4. Compression and heating of the chromosphere

The trajectories of “liquid particles” can be obtained by the numerical integration of Eq. (6) with respect to time. The degree of compression is simply defined by the change of the distance between two particles lying in the same trajectory and on neighboring field lines

$$\frac{\rho}{\rho_0} = -\frac{l_0}{l} \quad (11)$$

For simplicity, the vertical velocity of the current  $v_0$  will be assumed constant.

Fig. 5 shows the density distribution in elements initially located at the same height  $y = y_0$  in the chromosphere at sequential times. Enhanced density region ranges from  $x = h$  to the saddle point  $x = s$ . Density increases until the current reaches height comparable with  $s$ . It can be seen from (9) that at any given point  $x$ , electric field diminishes when  $h$  approaches the value of  $x$  and becomes zero at  $h = x$ . Maximum of density displays along the  $x$ -axis insignificantly. But looking at the density changes during time intervals between adjacent curves in Fig. 5, it can be seen (Fig. 6) that the region with compression moves in the direction of the  $x$  increase together with the saddle point, although the amplitude of the compression, of course, diminishes because of the decrease of the electric field source.

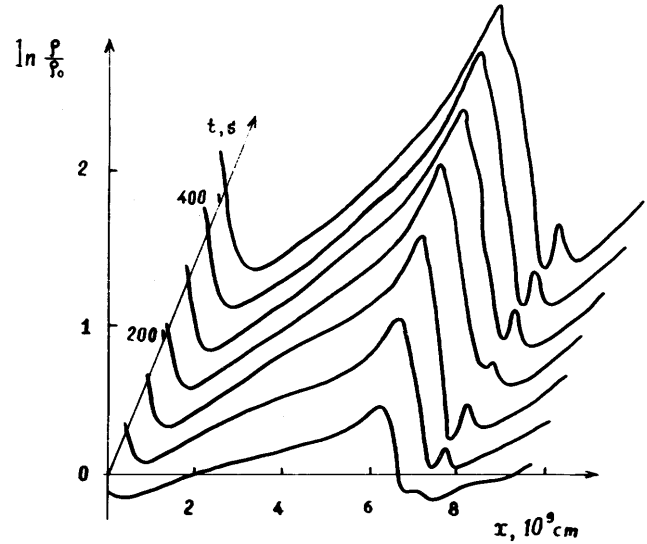


Fig. 5. Density variations  $\rho/\rho_0$  in the elements, arranged initially at the same height  $y_0 = 0.1d$  above the photosphere, at consecutive time moments. Ascending speed of the filament is 100 km/s

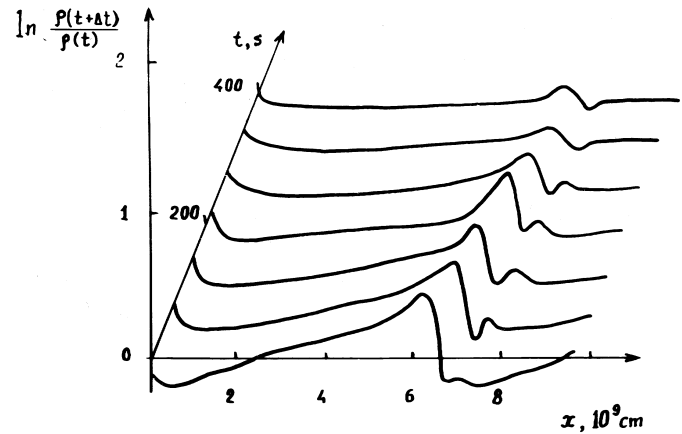


Fig. 6. Relative density variations  $\rho(t + \Delta t)/\rho(t)$  in the same elements as in Fig. 5,  $\Delta t = 50$  s

If there were no energy losses, the temperature in the compressed region would rise proportional to the 2/3 power of the density variation. But every temperature increase leads to enhanced emission which cools the plasma. The regions of enhanced emission in our model have the shape of ribbons parallel to the filament on both sides of it. In the parts of the ribbons closer to the filament, the emission will fade earlier than in the outer parts, because the compression ends there first, as Fig. 6 shows. Moreover, the outer boundaries move away from the filament. These two factors can result in the growing separation of the flare ribbons after the beginning of the eruption.

Of course, this analysis rather indicates the tendency for chromospheric response after a filament eruption than answers the question what is the radiation dynamics. It is necessary to do more rigorous calculations taking into consideration radiative losses, thermal conductivity, longitudinal motions etc. Never-

theless, even these rough estimates suggest that the filament eruption should have a pronounced effect on the radiation processes in the chromosphere.

## 5. Energy estimates

Observations of eruptive prominences show (Ballester, 1984; Molodenskij et al., 1992) that the current in them reaches  $10^{12}$  A. If eruption starts from a height  $10^9$  cm, the magnetic field in the region of compression is  $\approx 60$  gauss. The level in the chromosphere with the particle density  $n_0 = 10^{14}$   $\text{cm}^{-3}$  corresponds to the condition  $\beta = 8\pi nkT/B^2 = 1$  for this field. The number of particles within the column of the chromosphere above this level per unit area is

$$N = \int_0^\infty n_0 e^{-\frac{y}{H}} dy = n_0 H, \quad (12)$$

where  $H$  is the height of homogeneous atmosphere. Assuming  $H = 5 \cdot 10^7$  cm we obtain  $N = 5 \cdot 10^{21}$   $\text{cm}^{-2}$ . Two-ribbon flare area  $S$  is given by Allen (1973) as  $S = 3 \cdot 10^{19}$   $\text{cm}^2$ . As seen in Fig. 5 the maximum compression degree  $V_0/V$  ranges up to about 7. Assuming that compression is uniform in the  $x$  and  $y$  directions, the initial area in the chromosphere involved in the process is  $S_0 = S(V_0/V)^{1/2}$ , which gives  $8 \cdot 10^{19}$   $\text{cm}^2$ . The total amount of thermal energy contained in the quiet chromosphere above the level with  $n_0$  is

$$\varepsilon_0 = \frac{3}{2} N S_0 k T_0 = 10^{30} \text{ erg}. \quad (13)$$

From the ideal gas equation

$$\varepsilon = \frac{pV}{\gamma - 1} \quad (14)$$

and the adiabatic equation

$$pV^\gamma = \text{const} \quad (15)$$

we obtain

$$\varepsilon = \frac{\text{const}}{(\gamma - 1)V^{\gamma-1}}, \quad (16)$$

or

$$\varepsilon = \varepsilon_0 (V_0/V)^{\gamma-1}. \quad (17)$$

After the cooling of the compressed gas to the temperature  $T_0$ , its internal energy will be equal to  $\varepsilon_0$  again. So the energy that can be emitted during the cooling is

$$\Delta\varepsilon = \varepsilon - \varepsilon_0 = \varepsilon_0 [(V_0/V)^{\gamma-1} - 1] \approx 3 \cdot 10^{30} \text{ erg}. \quad (18)$$

This energy compares well with the energy emitted in the  $\text{H}\alpha$  line in a big flare.

## 6. Conclusions

The structure of the magnetic field in a model of inverse polarity, and field variations during the eruption, are such that frozen-in plasma motion produces regions of compression and rarefaction in the chromosphere. The compression regions take the shape of two belts parallelling the filament on each sides. The positions of the belts correspond to the flare ribbons. The belts move apart from a polarity inversion line as the filament ascends. This is consistent with the observed ribbon divergence with time.

Compression of the chromospheric gas by magnetic field must inevitably be accompanied by heating and emittance increase. The latter, as a matter of fact, is recorded as  $\text{H}\alpha$  flare. This mechanism is effective only in the initial stage of eruption; therefore, it has a short duration. As soon as the filament reaches the height comparable with the distance between the belts, the compression of the chromospheric matter becomes negligible.

The foregoing analysis is rather simplified. We only note the existence of regions in the chromosphere where plasma is compressed by magnetic field during the eruption and where therefore enhanced emission should arise. For more sophisticated treatment it is necessary to calculate the thermal balance taking into consideration conductive and radiative losses, longitudinal motion and so on.

*Acknowledgements.* I am grateful to the referee Dr. E.F. Hildner for his correction of the language of this paper. This work was supported in part by the Russian Foundation for Basic Research (grant 96-02-16285)

## References

- Anzer U., Pneuman G.W., 1982, *Sol. Phys.* 79, 129  
 Allen C.W., 1973, *Astrophysical Quantities*, The Athlone Press, 3rd ed.  
 Ballester J.L., 1984, *Sol. Phys.* 94, 151  
 Banin V.G., Fedorova A.S., 1971, in: *Issledovania po geomagnetizmu, aeronomii i fizike solntsa*, Vostochno-Sibirskoe Knizhnoe Izdatel'stvo, Irkutsk, V. 20, p.73  
 Filippov B.P., 1996, *A&A* 313, 277  
 Filippov B.P., Shilova N.S., 1995, *AZh* 72, 222  
 Hood A.W., Priest E.R., 1980, *Sol. Phys.* 66, 113  
 Kuperus M., Van Tend W., 1981, *Sol. Phys.* 71, 125  
 Martens P.C.H., Kuin N.P.H., 1989, *Sol. Phys.* 122, 263  
 Martin S.F., Ramsay H.E., 1972, in: *McIntosh P.S., Dryer M. (eds.) Solar Activity Observations and Predictions*, M.I.T. Press, Cambridge (Mass.), p.371  
 Molodenskij M.M., Filippov B.P., 1987, *AZh* 64, 1079  
 Molodenskij M.M., Filippov B.P., 1992, *Magnetic Fields of Solar Active Regions*, Nauka, Moscow  
 Molodenskij M.M., Filippov B.P., Shilova N.S., 1992, *AZh* 69, 181  
 Priest E.R., 1982, *Solar Magnetohydrodynamics*, Reidel, Dordrecht  
 Rust D.M., Bar V., 1973, *Sol. Phys.* 33, 445  
 Somov B.V., Syrovatskii S.I., 1971, *JETF*, 61, 621  
 Somov B.V., Syrovatskii S.I., 1974, in: *Neitralnye Tokovye Sloi v Plazme*, Nauka, Moscow, p. 14  
 Svestka Z., 1976, *Solar Flares*, Reidel, Dordrecht  
 Van Tend W., Kuperus M., 1978, *Sol. Phys.* 59, 115  
 Zirin H., Lackner D.K., 1969, *Sol. Phys.* 6, 86

This article was processed by the author using Springer-Verlag L<sup>A</sup>T<sub>E</sub>X A&A style file L-AA version 3.